

SYNCHRONOUS GLOBALLY OBSERVABLE ULTRASHORT-PERIOD PULSES

R.A. Marchuk

*Institute of Solar-Terrestrial Physics SB RAS,
Irkutsk, Russia, marchuk@mail.iszf.irk.ru*

A.S. Potapov

*Institute of Solar-Terrestrial Physics SB RAS,
Irkutsk, Russia, potapov@iszf.irk.ru*

V.V. Mishin

*Institute of Solar-Terrestrial Physics SB RAS,
Irkutsk, Russia, vladm@iszf.irk.ru*

Abstract. We have studied the properties of impulsive geomagnetic disturbances, which are observed synchronously at the network of induction magnetometers of the Institute of Solar-Terrestrial Physics (ISTP SB RAS) and Canadian stations of the CARISMA project [Mann, et al., 2008]. A feature of the pulses we detected is that their frequency range ($f \sim 5\text{--}30$ Hz) lies at the junction of the ranges of two known classes of electromagnetic oscillations: ultra-low-frequency (ULF) oscillations ($f < 5\text{--}10$ Hz), or geomagnetic pulsations, and extra-low frequency (ELF) oscillations ($f \sim 30\text{--}300$ Hz); therefore, the 5–30 Hz range is poorly studied. The work is of undoubted interest for physics of processes in the magnetosphere–ionosphere–atmosphere system. Morphological analysis of the pulses detected has been carried out using data from ISTP stations. As a result, we obtained statistical characteristics of the pulses, plotted their dynamic spectra, and determined a number of unusual properties that distinguish them, on the one hand, from geomagnetic pulsations of the pulsed type (irregular pulsations of the Pi1B type), and, on the other

hand, from higher frequency ELF and VLF signals (atmospherics, whistlers, etc.). On the basis of the results, we have made an assumption that a source of the pulses under study can be electrical sprites caused by powerful thunderstorms at middle and low latitudes. Using the results obtained by Wang, et al. in [2019] on spatial and temporal fixation of sprites in North China, we have confirmed that ultra-short-period pulses occur following the emergence of sprites. Thunderstorm activity, both local and global, is considered to be one of the main sources of excitation of the ionospheric Alfvén resonator (IAR), which plays an important role in coupling the ionosphere and the magnetosphere. The pulsed oscillations of interest may be one of the agents through which the energy of thunderstorms is transferred to IAR, thereby including the atmosphere in the system considered.

Keywords: geomagnetic pulsations, magnetosphere, ULF-ELF frequency range, red sprites, lightning, Alfvén resonator.

INTRODUCTION

Natural electromagnetic emission at the boundary of the ultra-low-frequency (ULF, 0.001–5 Hz) and extra- and very low-frequency (ELF/VLF, 3–300 Hz) ranges have not been studied in sufficient detail. For the present, the best known emissions in the frequency range 5–100 Hz are from the ionospheric Alfvén resonator (IAR) (see the review [Potapov et al., 2021]) with harmonic frequencies from fractions of hertz to 8–10 Hz and from the Schumann resonator (Earth–ionosphere) with a fundamental frequency of ~ 8 Hz. At the same time, electrical activity in the atmosphere, associated primarily with thunderstorms, is known to generate sufficiently powerful electromagnetic signals (spherics, atmospherics, tweaks, whistles) [Gershman, Ugarov, 1960]. Thunderstorm activity is diverse, and lightning discharges of different types generate pulses of different frequencies, some of which fall within the boundary range mentioned above. Energy of these pulses feeds waveguides and resonators, including IAR and the Schumann resonator. Of particular importance is the transfer of thunderstorm energy to IAR, which connects the ionosphere with the atmosphere on the one hand, and with the magnetosphere on the other.

Thunderstorms as sources of energy for IAR and the Schumann resonator emissions have been considered by

many authors [Belyaev et al., 1989; Fedorov et al., 2006; Nose et al., 2017]. But what thunderstorms can be the main supplier of energy for excitation of resonance atmospheric-ionospheric structures? This question needs to be answered.

In this paper, we study properties of impulsive geomagnetic disturbances observed synchronously at induction magnetometer networks of the Institute of Solar-Terrestrial Physics (ISTP SB RAS) and Canadian stations of CARISMA project [Mann et al., 2008], (Figure 1). Using data from Russian stations, we perform a morphological analysis of pulses detected and assume that their source may be electrical sprites [Wang et al., 2019] caused by powerful thunderstorms at middle and low latitudes. The possibility of feeding IAR oscillations through the energy of pulses detected is discussed.

1. OBSERVATIONS

We have used data from a combined network composed of stations of two networks. Location of these stations is shown in Figure 1; green circles mark ISTP SB RAS stations; red triangles indicate CARISMA stations. Geographic coordinates of these stations, models of the magnetometers installed, and their sample rates are listed in Table 1.

Table 1

Coordinates of the stations whose data is used in this paper

Observatory (station)	Geographic coordinates		Magnetometer sample rate, Hz	Magnetometer model
	φ	λ		
Istok (IST)	70.0	88.0	64	LEMI-30
Mondy (MND)	51.6	100.9	64	LEMI-30
Uzur (UZR)	53.1	107.4	40	LEMI-418
Ministik Lake (MSTK)	53.4	247.0	100	LEMI-30
Thief River Falls (THRF)	48.0	263.6	100	LEMI-30

Characteristics of the induction magnetometers are identical at all the stations, only their sample rates differ. Figure 2 plots the frequency response and the noise level of the LEMI-30 induction magnetometer at the station Mondy [http://lemisensors.com/wp-content/uploads/2018/03/LEMI-030_Datasheet.pdf]. Magnetometers at the stations of the CARISMA network have the same characteristics; for more details see [<http://www.carisma.ca/backgrounder/carisma-induction-coils>] and [Mann et al., 2008]. The magnetotelluric station LEMI-418 at the station Uzur is equipped, in addition to induction sensors, with a ferrosonde and LEMI-701 telluric current sensors. The induction part of the LEMI-418 station is identical to the LEMI-30 magnetometer.

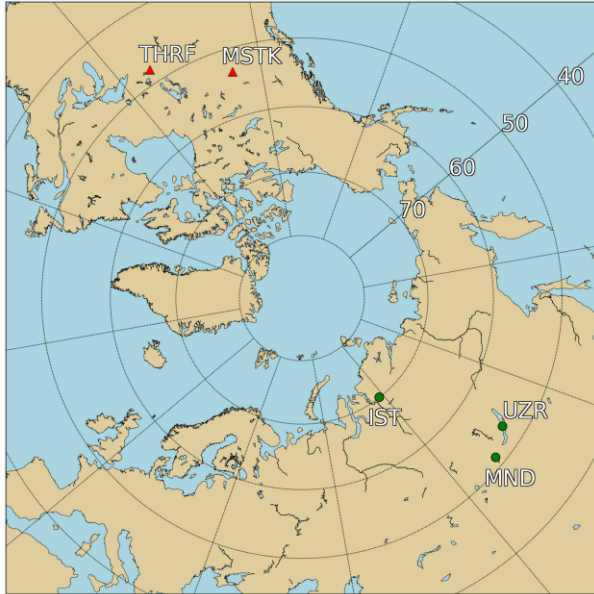


Figure 1. Map of stations whose data was used in the analysis

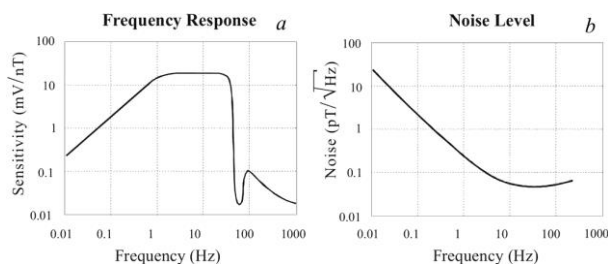


Figure 2. Frequency response (a) and noise level (b) of LEMI-30

1.1. Ultrashort-period pulses of the geomagnetic field

When analyzing data from the Integrated Magnetic-Ionospheric Observatory (IMIO) of ISTP SB RAS, we detected ultrashort-period pulses (USP) of the geomagnetic field, observed synchronously at the mid-latitude stations Mondy, Uzur, and at the high-latitude station Istok (Figure 3).

The typical form of the impulsive disturbances detected is a damped sinusoid with one intense pulse at the beginning (Figure 3, a). A form with several paired pulses is observed less frequently (Figure 3, b). A train of these pulsations can contain up to ten oscillations.

The double amplitude (peak-to-peak) of the pulses varies in the range $B \sim 0.001\text{--}0.1$ nT. The occurrence rate of the pulsations detected is extremely high; according to our data, it is about several tens (from 30 to 60) of pulses per 5 min, i.e. 6–12 pulses/min (Figure 4). Duration of one wave packet (train) is from 0.3 to 2 s.

The pulses under study usually retain the shape of the signal wave packet in the data from all the three stations; however, at the station Uzur in all cases detected, these oscillations are in antiphase compared to those obtained at the stations Istok and Mondy. We suspect that this is due to the incorrect installation of the X component sensor in the station Uzur.

Magnetic variations as an alternating magnetic field should induce electric currents in the earth. The relationship between telluric currents and geomagnetic pulsations was theoretically established as early as the middle of the last century in [Tikhonov, 1950; Cagniard, 1953]. The pulses detected also manifest themselves in telluric currents; for example, the station Uzur, simultaneously with USP in the geomagnetic field, observed disturbances of telluric currents (Figure 5).

2. MORPHOLOGICAL ANALYSIS OF PULSATIONS

To determine statistical characteristics of the pulses detected, we have analyzed USP recordings made at the IMIO stations on April 16, 2019. We took 5 min intervals that began at 01:30, 08:30, 11:25, 16:55, 19:10 UT and searched for USP in them. The criterion for the presence of USP was the synchronous occurrence of characteristic short-period disturbances, similar to those shown in Figure 3, at all three IMIO stations. As a result, we have found 152 USP events. Data and results of their preliminary analysis are available at

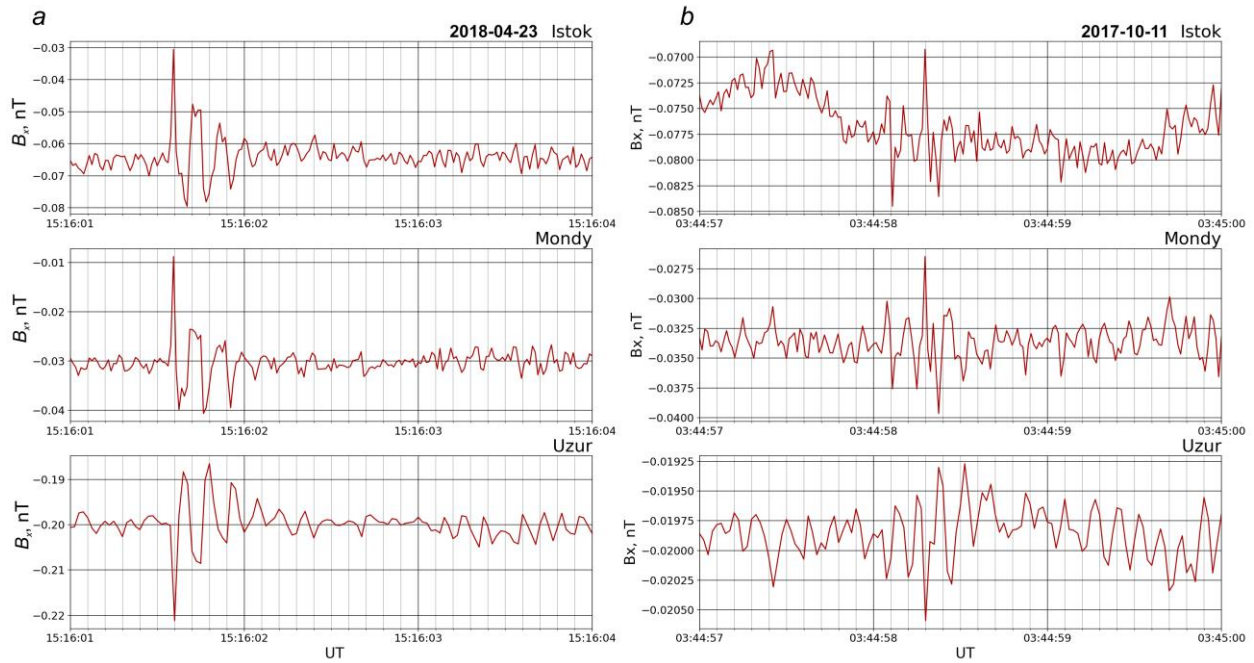


Figure 3. Examples of USP: oscillations in the form of a train on April 23, 2018 (a) and a paired pulse on October 11, 2017 (b)

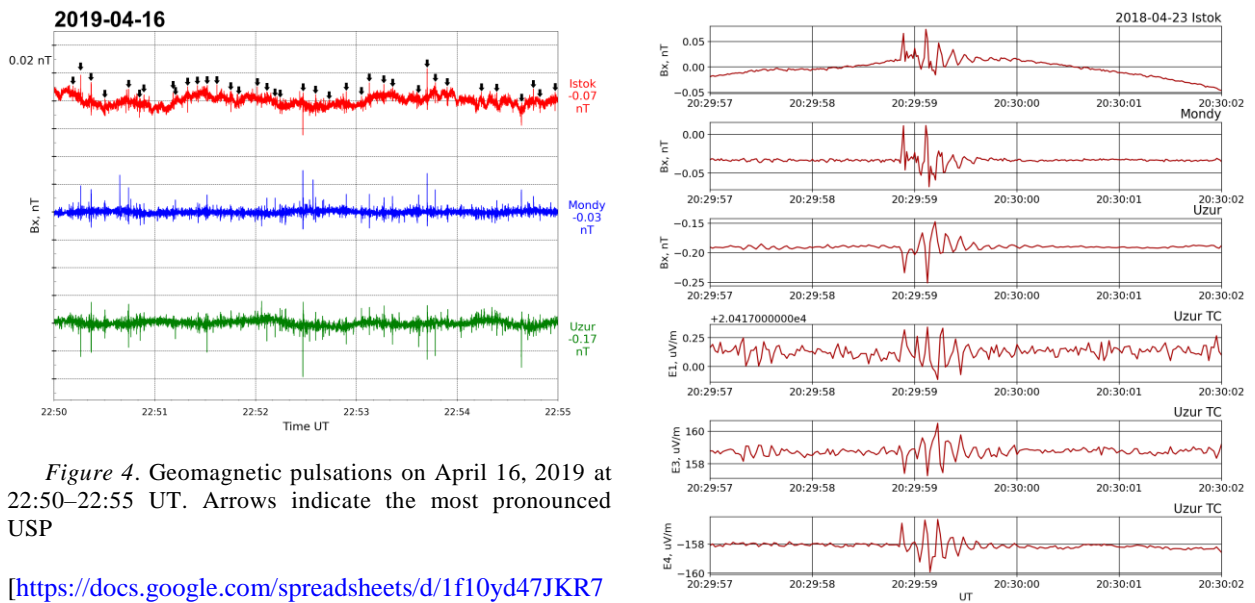


Figure 4. Geomagnetic pulsations on April 16, 2019 at 22:50–22:55 UT. Arrows indicate the most pronounced USP

[<https://docs.google.com/spreadsheets/d/1f10yd47JKR7FJ8HgUzIVI3bxfju2Utz0/edit?usp=sharing&ouid=108794281214343087703&rtfpof=true&sd=true>].

Time, signal duration, amplitudes at three stations, and the ratio between amplitudes measured at the mid-latitude (MND) and high-latitude (IST) stations are given.

The results obtained are presented in Figure 6 in the form of distributions of the number of events over their amplitude (a), duration (b), and ratio between the amplitudes at the stations Mondy and Istok (c).

As mentioned above, duration of the pulses ranges from 0.3 to 2 s, while in 77 % of cases it falls within 0.3–0.8 s. The mean and median are about 0.7 s. The amplitude distributions (everywhere we mean the range of oscillations in a pulse, or the so-called double amplitude) at the stations Istok and Mondy have a sharp peak corresponding to the intervals 12–14 and 10–14 pT respectively.

It also includes medians of the amplitude distributions. The average amplitudes are shifted toward their

Figure 5. Disturbances of the geomagnetic field and telluric currents on April 23, 2018: three top panels show the B_x component at the IMIO stations, three bottom panels are variations in electric field components from recordings of telluric current sensors at the station Uzur

higher values: ~16 pT at the station Istok and 18 pT at the station Mondy. At the station Uzur, the amplitude distribution is more diffuse, and the average value is 20.5 pT. It is interesting to compare the USP amplitudes obtained at the stations Mondy and Istok. Figure 6, c illustrates the distribution of the logarithm of the amplitude ratio at these stations. The cases when the amplitude at one station exceeds the amplitude at another are seen to be almost equally probable.

Nonetheless, the question about the USP amplitude ratio at different points of Earth’s surface is not as simple as it might seem. With the frequency range of the pulses,

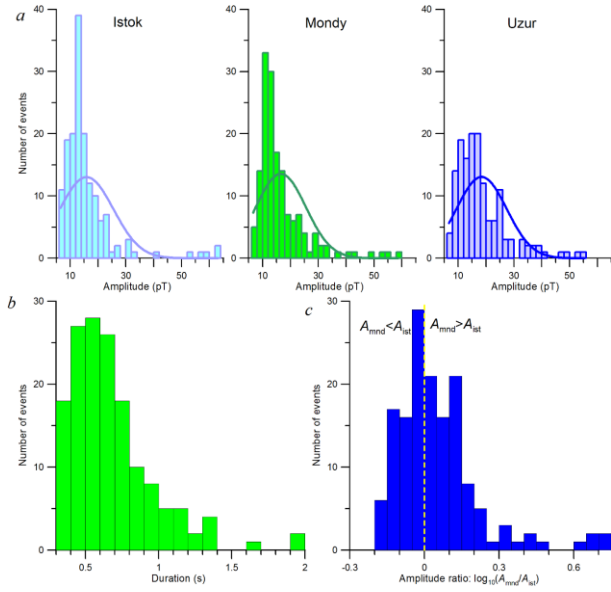


Figure 6. Statistical characteristics of USP obtained from the results of the morphological analysis for April 16, 2019

they can be considered as short-term perturbations of modes (standing waves) of the Schumann resonator. These modes, or harmonics, in the horizontal direction have alternating nodes and antinodes, the distance between which depends on the harmonic number [Satori et al., 2012; <http://janto.ru/repository/008/annex-b.html>]. The USP amplitude measured on the ground is likely to depend on the phase of a standing wave at the measurement point, i.e. it will

be maximum at antinodes and minimum or zero at nodes. In this article, we do not delve into the interaction between the pulses observed and the Schumann resonator modes; their analysis requires further investigations.

To analyze the energy distribution over the frequencies of the pulses analyzed, we have plotted dynamic spectra, using the wavelet analysis (Figure 7).

The spectra show that the main energy of the pulsations is in the frequency range 4–32 Hz. In this case, maxima correspond to frequencies of 8, 14, 20, and 26 Hz, which are close to the harmonic frequencies of the Schumann resonance.

The closest analogue of the USP considered in the range of geomagnetic pulsations are Pi1B pulsations, which are excited and propagate in the ionosphere during precipitation of energetic charged particles in the region of maximum intensity of the westward electrojet [Parkhomov, Rakhmatulin, 1975]. Pi1B have a periodic spectrum structure similar to USP, but their frequency range is at lower frequencies 0.1–5 Hz. In terms of the train duration, the USP events of interest are much shorter (≤ 2 s) than the Pi1B pulsations lasted for ≤ 1 –10 min. In addition, the occurrence rate of Pi1B is much lower than that of USP. The Pi1B pulsations depend on auroral activity, appear during periods of its intensification, occur most often in the auroral zone; and in middle latitudes, only during powerful disturbances (magnetic storms) [Mishin et al., 2020]. The analysis did not reveal any correlation between USP and

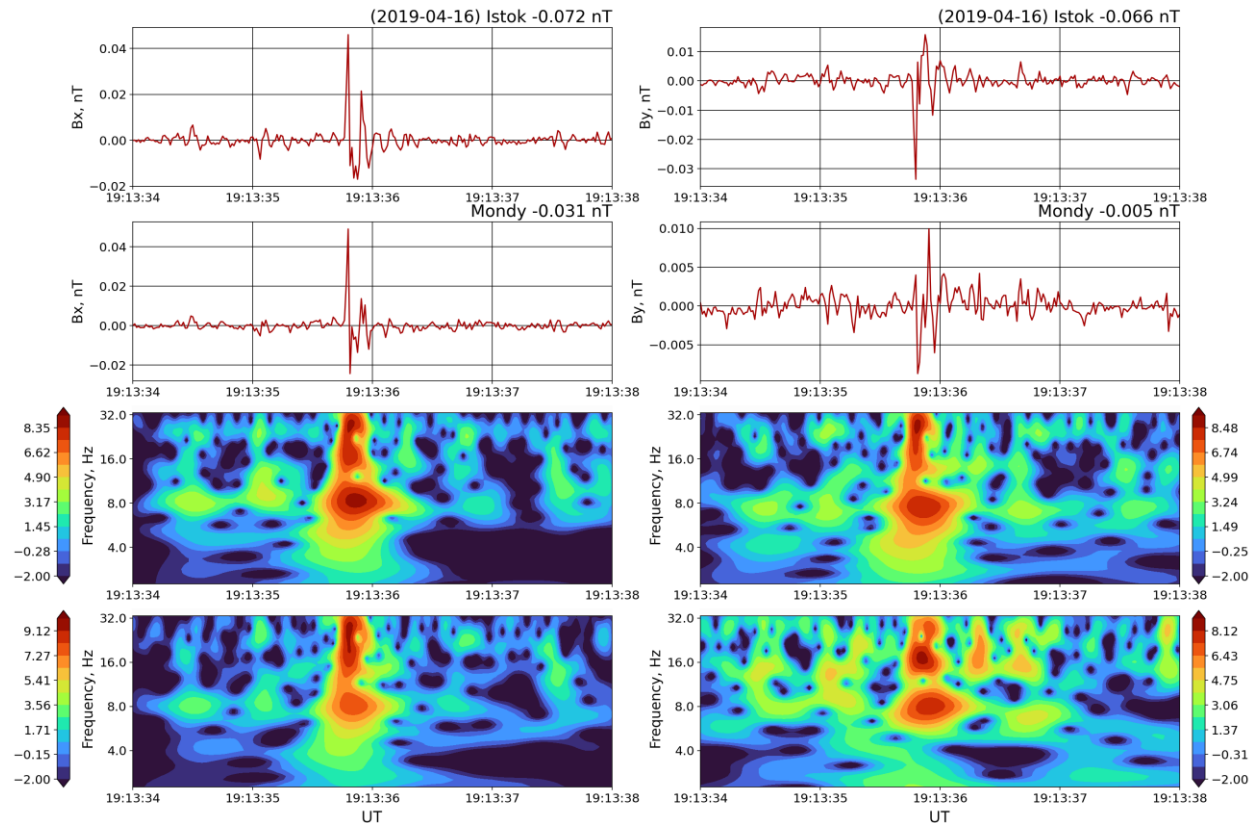


Figure 7. USP in B_x (two top left panels) and B_y (two top right panels) observed at the stations Istok and Mondy on April 16, 2019 at 19:13:36 UT, and associated dynamic spectra (third and fourth panels from the top)

geomagnetic activity. Based on the facts described above, we can confidently assert that the USP events considered differ morphologically and genetically from irregular geomagnetic pulsations.

3. ANALYSIS OF USP OBSERVATIONS AT DIFFERENT LONGITUDES

To study the extent of USP propagation in longitude, we have analyzed observations made at a wide network of ground stations, using data from the Canadian network CARISMA (Canadian Array for Realtime Investigations of Magnetic Activity). We chose data from the stations Ministik Lake (MSTK) and Thief River Falls (THRF) located in the Western Hemisphere in the sector opposite in longitude to the ISTEP SB RAS stations.

The analysis of observations for February 17, 2019 has revealed the presence of synchronous pulses in the geomagnetic field at the stations of the CARISMA and ISTEP SB RAS networks (Figure 8). We have studied the delays between the first USP extrema at these stations for about 20 most intense USP events: they varied from 0 (taking into account the finiteness of sampling intervals) to 30 ± 20 ms. It should be considered that the sample rate of induction magnetometers differs at the ISTEP SB RAS and CARISMA stations, and USP trains might be subject to distortions at such large distances due to the influence of the Earth–ionosphere waveguide, resulting in that the peaks can move apart and come together, and the delay may increase.

With allowances made for the high degree of synchronism of USP occurrence at the global network of stations, it is reasonable to assume that the signals propagate at the speed of light or close to it, and lightning discharges in thunderstorm cells can be the source of pulses. Such cells are located in equatorial regions, and thunderstorm activity in them is constant.

Using data from [Christian et al., 2003], we selected points in the regions described above, where thunderstorm flashes happen most often. In this case, they should be the most common generation source of USP. Next, we obtained the distance from these points to the stations

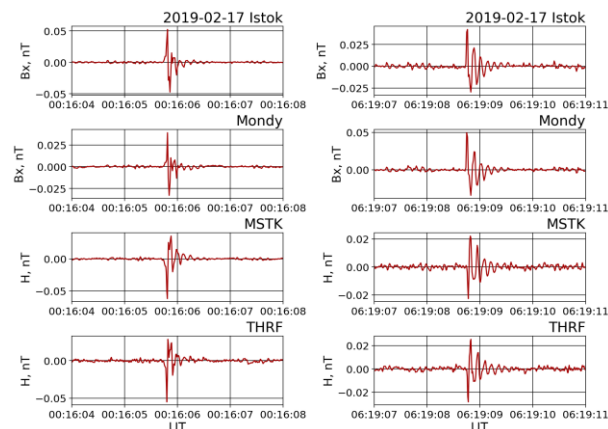


Figure 8. Two examples of USP events observed at four stations on February 17, 2019

selected, using the Mathematica software package with-GeoDistance function, which computes the distance between points on Earth from their coordinates in the ideal ellipsoid approximation. Then we calculated the theoretical minimum propagation time of USP, assuming the propagation velocity equal to the velocity of light, and the delays compared to the minimum propagation time for each station.

The results obtained show (Table 2) that signals during propagation of emission at the velocity of light are detected at the limit of the magnetometer resolving power. When thunderstorms occur in South America or Asia, we can still see the delay between USP events, but during thunderstorms in Africa or at higher latitudes than those taken for calculations in Table 2 with the available temporal resolution USP events will be recorded synchronously at all stations employed. Note, however, that all the delays obtained are positive or zero, which is quite understandable. In fact, signals propagate not strictly along Earth’s surface, but above, reflecting alternately from Earth and the ionosphere.

Another interesting question arises here. Judging from the comparison between amplitudes of synchronous pulses at different stations, attenuation of signals is very low. Why then is there no effect of a round-the-world echo in this case? Probably because it is very difficult to detect such an effect with the existing waveform: the signal travel time around Earth (~ 0.13 s) is comparable to the pulse duration (0.3–2 s) and the repeated signal is lost against the pulse tail. Yet the occasionally observed double pulses (see Figure 1, *b*) may well be a manifestation of the round-the-world echo, but this issue requires additional consideration.

1. RELATIONSHIP BETWEEN USP AND GLOBAL THUNDERSTORM ACTIVITY

Generation of geomagnetic pulsations close to the range under study — Schumann resonances and IAR emission — during thunderstorm activity has been studied in [Surkov et al., 2006; Fedorov et al., 2006]. It has been experimentally analyzed in [Schekotov et al., 2011]. These papers deal only with the generation of pulsations from nearby thunderstorms, whereas the contribution from distant thunderstorms is considered insignificant. The USP events we observe also occur with the same frequency in winter periods when there is no thunderstorm activity in the Northern Hemisphere at middle and high latitudes. We therefore put forward an assumption that the generation source of the pulsations detected is in the equatorial zone, where constant zones of powerful thunderstorms are located [Blakeslee et al., 2014].

Lightning discharges caused by a large electric potential gradient, which produces a strong electric field, generate powerful electromagnetic pulses. These pulses are called atmospheric, or spherics. They can propagate for many kilometers through the waveguide between the lower ionosphere and Earth’s surface. A maximum

Table 2

Results of calculations of the propagation time of emission from zones of increased thunderstorm activity

Point (-27.75° , -56.25°): South America, Posadas, Argentina			
Station	Distance to station, thousand km	Theoretical minimum time of distribution, ms	Delay compared to the minimum propagation time, ms
Istok	14.8	49.3	18.25±15.6
Mondy	16.7	55.8	24.76±15.6
Uzur	16.9	56.3	25.23±25
Ministik Lake	10.5	35.2	4.07±10
Thief River Falls	9.3	31.1	0±10
Point (-1.25° , 27.75°): Africa, Kamembe, Ruanda			
Istok	9	30.20	0.30±15.6
Mondy	8.9	29.90	0±15.6
Uzur	9.4	31.46	1.55±25
Ministik Lake	13.2	44.00	14.10±10
Thief River Falls	12.5	41.94	12.03±10
Point (3.25° , 101.75°): Asia, Kuala Lumpur, Malaysia			
Istok	9	24.92	7.05±15.6
Mondy	8.9	17.87	0±15.6
Uzur	9.4	18.51	0.64±25
Ministik Lake	13.1	43.09	25.22±10
Thief River Falls	12.5	46.80	28.93±10

propagation distance of spherics may be as large as several thousand kilometers [Shvets et al., 2015]. If the spherics seep through the ionosphere along geomagnetic field lines (also known as whistlers), they can propagate to even greater distances, if not to polar latitudes [Gershman, Ugarov, 1960; Allcock, 1960]. The main part of the energy of spherics lies in ELF (30–300 Hz) and VLF (3–30 kHz) ranges, i.e. the emission frequency of spherics and whistling atmospherics is much higher than the ULF range.

The choice of lightning discharges as a source of USP can explain their high occurrence rate, the global scale of observation, and the propagation velocity. Yet, according to satellite data, the occurrence rate of lightning discharges all over Earth's atmosphere $\leq 44 \pm 5$ s $^{-1}$, and in general $\sim 1.4 \cdot 10^9$ lightnings occur per year [Encyclopedia..., 2005], which is by an order of magnitude higher than the occurrence rate of USP (6–12 pulses/min). Consequently, not all lightning discharges trigger USP events.

After analyzing literature on the frequency range of lightning discharges of different types, we have figured out that the closest to the USP range is the frequency range excited by lightnings of a special type, the so-called red sprites. These are lightning discharges in the upper atmosphere at altitudes from 40 to 100 km [Rodger, 1999], initiated by strong positive cloud-to-ground discharges [Huang et al., 1999; Price et al., 2002; Williams et al., 2007]. Duration of luminosity of sprites is usually equal to several milliseconds, but lu-

minosity of individual parts of a sprite might exceed 100 ms [Lu et al., 2013]. The time delay with respect to the beginning of a triggering lightning ranges from ~ 3 ms [Winckler, 1995] to several tens of milliseconds [Fukunishi et al., 1995], and according to observations [Wang et al., 2019] it may be as long as hundreds of milliseconds.

As inferred from [Paras, Rai, 2012], the main emission range of red sprites is at frequencies to 300 Hz with a maximum emission at 40 Hz. The sprite occurrence rate according to [Price, 2016] is of the order of several sprites per minute. These characteristics are much closer to those of USP.

4.1. Analysis of the relationship between ultrashort pulses and red sprites

To test the assumption about USP generation by red sprites, we have used the article [Wang et al., 2019] that recorded the time of occurrence of red sprites based on simultaneous observations at two stations in North China. The sprites were detected at 15:29:11.2815, 15:40:19.1388, 15:48:58.4567, 15:57:27.6660, 16:00:28.6739, and 17:29:50.5918 UT. Comparing the results with the data on pulsations from the stations Istok, Mondy, and MSTK, we have found that after each of the six cases of detection of red sprites analyzed in [Wang et al., 2019] USP events are observed at the stations of our integrated network. This is seen in Figure 9, where dashed red lines show the moments of occurrence of red sprites.

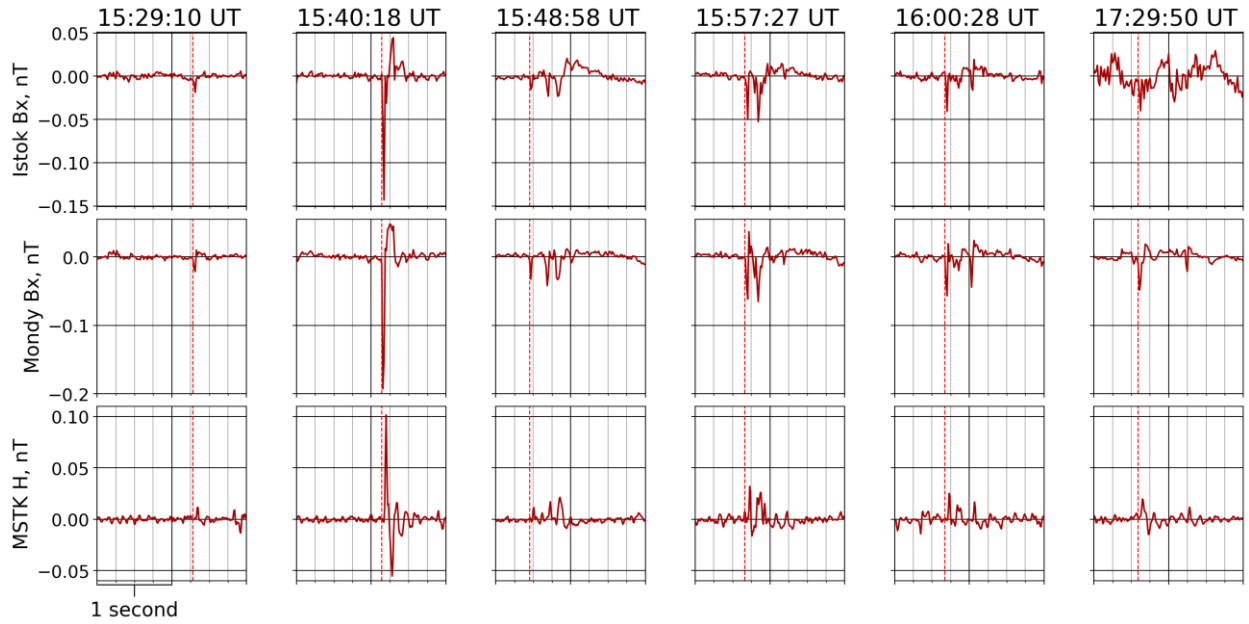


Figure 9. USP events observed at the stations Istok, Mondy, and MSTK after the sprites recorded in North China on August 8, 2017 [Wang et al., 2019]

Of principal interest is the second event in which a sprite in the form of a jellyfish was observed with peak current of the first discharge. It caused USP with an amplitude of ~ 0.2 nT. Such a large amplitude is usually typical of slow geomagnetic pulsations with minute periods associated with the development of geomagnetic activity, and not of short-period pulsations. Such USP events with an amplitude of ~ 0.1 nT can be recorded several times per 5 min. The characteristic USP amplitudes (~ 20 pT depending on station), described above in the section Morphological Analysis, occur when less powerful red sprites emerge (events 1, 3–6).

It is difficult to determine the exact delay between USP and the occurrence of red sprites due to the low resolution of induction magnetometers, and also because it is difficult to determine the beginning of USP against noise in geomagnetic pulsation data. It can, however, be estimated that the delay is several tens of milliseconds. For example, for event 2 the time between the occurrence of a red sprite and the first peaks of an oscillation train at the stations Istok, Mondy, and MSTK were 32.8 ± 15.6 , 17.2 ± 15.6 , and 61 ± 10 ms respectively. The event coordinates are the following (see Figure 7 in [Wang et al., 2019]): 40.4° N, 116.7° E. The theoretical estimate of the delay for this event is, therefore, 12.3, 5.8, and 28.6 ms respectively. Thus, for the nearest station, Mondy, according to our estimates, the delay falls within the measurement uncertainty interval of 1.6 to 32.8 ms; in the most distant station, MSTK, the delay is already far from the corresponding uncertainty interval 51–71 ms. In all cases, the value lies below the measurement uncertainty interval or in its lower part, i.e. the signal propagation velocity is lower than the velocity of light, and the greater the distance, the more noticeable the difference (the same can be seen in Table 2).

This suggests that the process of signal propagation is not similar to the simple pulse transfer at a constant

speed in a homogeneous medium. In reality, we are dealing with propagation of an impulsive disturbance in a spherical inhomogeneous waveguide, which is also the Schumann resonator. The problem is that we do not know how the pulse as a set of frequencies improper for the resonator interacts with eigenmodes of the resonator. This question warrants serious theoretical consideration. Our paper provides some empirical material for such work.

In summing up, we should note that all six cases of electric sprites from [Wang et al., 2019] resulted in USP. Unfortunately, we are unable to conduct a rigorous statistical analysis of the relationship between sprites and USP due to lack of additional observational data on sprites. We can conclude that it is very likely that all sprites generate USP, but we cannot say whether all USP events originate from sprites.

CONCLUSION

We have detected and analyzed ultrashort-period pulsations observed synchronously at a network of induction magnetometer stations at middle and high latitudes. We have carried out a morphological analysis of more than 150 cases of USP observation and obtained their statistical characteristics. The spectra of the pulsations were examined. Then, we extended the survey coverage along the parallel to the Western Hemisphere. An assumption has been put forward that the source of the pulses under study is thunderstorms. After analyzing the literature on this topic, we assumed that the source of USP is not any lightning discharges, but red sprites that occur during especially powerful thunderstorms whose emission is in a range close to the USP range. We have found that USP events occur after each red sprite recorded by Wang et al. [2019] in North China.

As a continuation of this work, attention should be paid to the classification of USP events and to the iden-

tification of characteristic morphological properties of individual USP subtypes. It is also of interest to study the degree of attenuation of these pulses depending on the state of the Earth–ionosphere waveguide. It is also useful to try to find cases of round-the-world echoes of such pulses (which should be observed with such small amplitude damping). Besides, in order to reveal the correlation between USP characteristics with the time of day and geomagnetic activity, it is necessary to learn how to identify USP automatically by correlation methods. It is also necessary to compare USP with a large number of globally observable red sprites and to study the relationship between USP and other lightning discharges of the upper atmosphere such as blue jets and elves.

The findings provide new information about redistribution of thunderstorm energy in the atmosphere and its partial transfer to waveguide atmospheric-ionospheric structures. Thus, the fact that USP spectral maxima coincide with the harmonic frequencies of the Schumann resonator clearly indicates that the pulses we detected feed oscillations in this resonator. We can assume that further this energy can flow both into IAR and into the magnetosonic waveguide in the F2 layer of the ionosphere. There is a lot of evidence, both theoretical and experimental, of a close link and interaction between the above mentioned waveguide and resonant structures [Lysak, Yoshikawa, 2006; Potapov et al., 2021].

The study was financially supported by the Russian Science Foundation (Grant No. 22-27-00280).

One of the authors (R.A.M.) is sincerely grateful to his first supervisor R.A. Rakhmatulin (1947–2020) for posing the problem and helping with data analysis at the first stages of the study. We thank R.V. Vasiliev and A.V. Oinats for useful discussions.

We are indebted to the organizers and operators of the Canadian network CARISMA and personally to Drs I.R. Mann, D.K. Milling for providing induction magnetometer data. CARISMA is managed by the University of Alberta and funded by the Canadian Space Agency.

REFERENCES

- Allcock G.McK. Propagation of Whistlers to Polar Latitudes. *Nature*. 1960, vol. 188, pp. 732–733. DOI: [10.1038/188732a0](https://doi.org/10.1038/188732a0).
- Belyaev P.P., Polyakov S.V., Rapoport V.O., Trakhtengerts V.Y. Theory for the formation of resonance structure in the spectrum of atmospheric electromagnetic background noise in the range of short-period geomagnetic pulsations. *Radiophys. Quantum Electron*. 1989, vol. 32, no. 7, pp. 594–601.
- Blakeslee R.J., Mach D.M., Bateman M.G., Bailey J.C. Seasonal variations in the lightning diurnal cycle and implications for the global electric circuit. *Atmos. Res*. 2014, vol. 135–136, pp. 22–243. DOI: [10.1016/j.atmosres.2012.09.023](https://doi.org/10.1016/j.atmosres.2012.09.023).
- Cagniard L. Basic theory of the magnetotelluric method of geophysical prospecting. *Geophys*. 1953, vol. 18, no. 3, pp. 605–635.
- Christian H.J., Blakeslee R.J., Boccippio D.J., Boeck W.L., Buechler D.E., Driscoll K.T., et al. Global frequency and distribution of lightning as observed from space by the optical transient detector. *J. Geophys. Res*. 2003, vol. 108, iss. D1, pp. ACL4-1–ACL4-15. DOI: [10.1029/2002JD002347](https://doi.org/10.1029/2002JD002347).
- Encyclopedia of World Climatology. Springer, 2005, 854 p. DOI: [10.1007/1-4020-3266-8](https://doi.org/10.1007/1-4020-3266-8).
- Fedorov E., Schekotov A.Ju., Molchanov O.A., Hayakawa M., Surkov V.V., Gladichev V.A. An energy source for the mid-latitude IAR: World thunderstorm centers, nearby discharges or neutral wind fluctuations? *Physics and Chemistry of the Earth*. 2006, vol. 31, pp. 462–468. DOI: [10.1016/j.pce.2006.02.001](https://doi.org/10.1016/j.pce.2006.02.001).
- Fukunishi H., Takahashi Y., Kubota M., Sakanoi K., Inan U.S., Lyons W.A. Lower ionospheric flashes induced by lightning discharges. *EOS Supplement*. 1995, vol. 46, p. F114.
- Gershman B.N., Ugarov V.A. Propagation and generation of low-frequency electromagnetic waves in the upper atmosphere. *Physics-Uspeski* [Advances in Physical Sciences]. 1960, vol. 72, pp. 235–271. (In Russian). DOI: [10.1070/PU1961v003n05ABEH005809](https://doi.org/10.1070/PU1961v003n05ABEH005809).
- Huang E., Williams E., Boldy R., Heckman S., Lyons W., Taylor M., et al. Criteria for sprites and elves based on Schumann resonance observations. *J. Geophys. Res.: Atmos*. 1999, vol. 104, no. D14, pp. 16943–16964. DOI: [10.1029/1999JD900139](https://doi.org/10.1029/1999JD900139).
- Lu G., Cummer S.A., Li J., Zigoneanu L., Lyons W.A., Stanley M.A., et al. Coordinated observations of sprites and in-cloud lightning flash structure. *J. Geophys. Res.: Atmos*. 2013, vol. 118, no. 12, pp. 6607–6632. DOI: [10.1002/jgrd.50459](https://doi.org/10.1002/jgrd.50459).
- Lysak R.L., Yoshikawa A. Resonant cavities and waveguides in the ionosphere and atmosphere. *Geophysical Monograph Series*. 2006, vol. 169, pp. 289–306. DOI: [10.1029/169GM19](https://doi.org/10.1029/169GM19).
- Mann I.R., Milling D.K., Rae I.J., Ozeke L.G., Kale A., Kale Z.C., et al. The upgraded CARISMA magnetometer array in the THEMIS era. *Space Sci. Rev*. 2008, vol. 141, pp. 413–451. DOI: [10.1007/s11214-008-9457-6](https://doi.org/10.1007/s11214-008-9457-6).
- Mishin V.V., Tsegmed B., Klibanova Y.Y., Kurikalova M.A. Burst geomagnetic pulsations as indicators of substorm expansion onsets during storms. *J. Geophys. Res.: Space Phys*. 2020, vol. 125, iss. 10, 15 p. DOI: [10.1029/2020JA028521](https://doi.org/10.1029/2020JA028521).
- Nose M., Uyeshima M., Kawai J., Hase H. Ionospheric Alfvén resonator observed at low-latitude ground station, Muroto. *J. Geophys. Res.: Space Phys*. 2017, vol. 122, no. 7, pp. 7240–7255. DOI: [10.1002/2017JA024204](https://doi.org/10.1002/2017JA024204).
- Paras M., Rai J. Electrical parameters of red sprites. *Atmosfera*. 2012, vol. 25, no. 4, pp. 371–380.
- Parkhomov V.A., Rakhmatulin R.A. Localization of Pi1B source. *Issledovaniya po geomagnetizmu, aeronomii i fizike Solntsa* [Research on Geomagnetism, Aeronomy and Solar Physics]. 1975, vol. 36, pp. 132–138. (In Russian).
- Potapov A.S., Polyushkina T.N., Tsegmed B. Morphology and diagnostic potential of the ionospheric Alfvén resonator. *Solar-Terr. Phys*. 2021, vol. 7, no. 3, pp. 36–52. DOI: [10.12737/stp-73202104](https://doi.org/10.12737/stp-73202104).
- Price C. ELF electromagnetic waves from lightning: The Schumann resonances. *Atmosphere*. 2016, vol. 7, no. 116, 20 p. DOI: [10.3390/atmos7090116](https://doi.org/10.3390/atmos7090116).
- Price C., Asfur M., Lyons W., and Nelson T. An improved ELF/VLF method for globally geolocating sprite-producing lightning. *Geophys. Res. Lett*. 2002, vol. 29, no. 3, pp. 1-1–1-4. DOI: [10.1029/2001GL013519](https://doi.org/10.1029/2001GL013519).
- Rodger C.J. Red sprites, upward lightning, and VLF perturbations. *Rev. Geophys*. 1999, vol. 37, no. 3, pp. 317–336. DOI: [10.1029/1999RG900006](https://doi.org/10.1029/1999RG900006).
- Satori G., Mushtak V., Neska M., Nagy T., Barta V. Global lightning dynamics deduced from Schumann resonance frequency variations at two sites ~550 km apart. *Geophys. Res. Abstr*. 2012, vol. 14, EGU2012-10647.
- Schekotov A., Pilipenko V., Shiokawa K., Fedorov E. ULF impulsive magnetic response at mid-latitudes to lightning activity. *Earth and Planetary Physics*. 2011, vol. 63, no. 2, pp. 119–128. DOI: [10.5047/eps.2010.12.009](https://doi.org/10.5047/eps.2010.12.009).
- Shvets A.V., Krivonos A.P., Serdiuk T.N., Goryshnya Y.V. Evaluating parameters of conductivity profile of the lower ionosphere by tweek-atmospherics. *Radiofiz. elektron*. 2015, vol. 20,

pp. 40–47. (In Russian). DOI: 10.15407/rej2015.01.040.

Surkov V.V., Hayakawa M., Schekotov A.Y., Fedorov E.N., Molchanov O.A. Ionospheric Alfvén resonator excitation due to nearby thunderstorms. *J. Geophys. Res.* 2006, vol. 111, iss. A1, 13 p. DOI: [10.1029/2005JA011320](https://doi.org/10.1029/2005JA011320).

Tikhonov A.N. On the determination of the electrical characteristics of the deep layers of the earth's crust. *Doklady Akademii nauk SSSR [Proceedings of the USSR Academy of Sciences]*. 1950, vol. 73, no. 2, pp. 295–297. (In Russian).

Wang Y., Lu G., Ming M., Zhang H., Fan Y., Liu G., et al. Triangulation of red sprites observed above a mesoscale convective system in North China. *Earth and Planetary Physics*. 2019, vol. 3, pp. 111–125. DOI: [10.26464/epp2019015](https://doi.org/10.26464/epp2019015).

Williams E., Downes E., Boldi R., Lyons W., Heckman S. Polarity asymmetry of sprite-producing lightning: A paradox? *Radio Sci.* 2007, vol. 42, no. 2, 15 p. DOI: [10.1029/2006RS003488](https://doi.org/10.1029/2006RS003488).

Winckler J.R. Further observations of cloud-ionosphere electrical discharges above thunderstorms. *J. Geophys. Res.: Atmos.* 1995, vol. 100, no. D7, pp. 14335–14345. DOI: [10.1029/95JD00082](https://doi.org/10.1029/95JD00082).

URL: http://lemisensors.com/wp-content/uploads/2018/03/LEMI-030_Datasheet.pdf (accessed March 30, 2022).

URL: <http://www.carisma.ca/backgrounder/carisma-induction-coils> (accessed March 30, 2022).

URL: <https://docs.google.com/spreadsheets/d/1f10yd47JKR7FJ8HgUzIVl3bxfju2Utz0/edit?usp=sharing&ouid=108794281214343087703&rtfpof=true&sd=true> (accessed March 30, 2022).

URL: <http://janto.ru/repository/008/annex-b.html> (accessed March 30, 2022).

Original Russian version: R.A. Marchuk, A.S. Potapov, V.V. Mishin, published in *Solnechno-zemnyaya fizika*. 2022. Vol. 8. Iss. 2. P. 52–60. DOI: [10.12737/szf-82202207](https://doi.org/10.12737/szf-82202207). © 2022 INFRA-M Academic Publishing House (Nauchno-Izdatelskii Tsentr INFRA-M)

How to cite this article

Marchuk R.A., Potapov A.S., Mishin V.V. Synchronous globally observable ultrashort-period pulses. *Solar-Terrestrial Physics*. 2022. Vol. 8. Iss. 2. P. 47–55. DOI: [10.12737/stp-82202207](https://doi.org/10.12737/stp-82202207).